

Energy straggling of protons through thin solid foils

D. G. Arbó, M. S. Gravielle, and J. E. Miraglia

*Instituto de Astronomía y Física del Espacio, Consejo Nacional de Investigaciones Científicas y Técnicas, Casilla de Correos 67,
Sucursal 28, 1428 Buenos Aires, Argentina*

and Departamento de Física, FCEN, Universidad de Buenos Aires, Buenos Aires, Argentina

J.C. Eckardt, G.H. Lantschner, M. Famá, and N.R. Arista

Centro Atómico Bariloche, Instituto Balseiro, 8400 Bariloche, Argentina

(Received 7 September 2001; published 12 March 2002)

The energy straggling of protons penetrating thin foils is theoretically and experimentally investigated for intermediate and high impact velocities. We calculate separately the contributions due to the interaction of the projectile with valence and core electrons. The energy straggling originated in the valence band is evaluated within the dielectric formalism, using the Mermin-Lindhard dielectric response function. The contribution coming from the core ionization is calculated with the continuum-distorted-wave-eikonal-initial-state (CDW-EIS) approximation. The predictions of the model are compared with recent measurements for Al, Zn, and Au targets. In addition, experimental results of straggling for Si are presented. The transmission method is used to measure the straggling, and experimental data are corrected to consider roughness effects. Theoretical values are in good agreement with the experiments in the whole range of energies considered. At low energies the binary interaction with valence electrons is the dominant mechanism, while the inner-shell contribution becomes the most important one as the energy increases.

DOI: 10.1103/PhysRevA.65.042901

PACS number(s): 34.50.Dy, 34.50.Bw

I. INTRODUCTION

When an ion beam penetrates matter it experiences a random set of collisions with valence electrons and atomic cores of the solid. As a result of these collisions the beam of particles spreads in energy. The parameter that describes this effect is called energy *straggling*, and is usually defined as the square root of the mean square deviation of the energy distribution.

In the present work, the energy straggling per unit path Ω is investigated, both theoretically and experimentally, for protons moving inside different solids. We analyze the intermediate and high impact energy range. Concerning the experimental values, in this paper we extend recent measurements [1] of energy straggling in various solids to Si targets. Since the topography of the sample plays an important role in the determination of Ω , experimental values obtained with the transmission method are corrected to discount foil roughness effects.

The work is organized as follows. In Sec. II the theoretical models used to calculate valence and core contributions to the energy straggling are outlined. The experimental technique and the correction employed to take into account the roughness effect of the sample are described in Sec. III. In Sec. IV results are shown and discussed, and Sec. V contains our conclusions. Atomic units are used unless otherwise stated.

II. THEORY

When a projectile with charge Z_p penetrates into a solid with velocity v , it loses energy as a consequence of collisions with electrons of the material. These collisions have a statistical nature and produce a dispersion in the projectile

energy. The dispersion of the ion energy can be determined through Ω^2 , which is defined as the mean square deviation of the energy distribution per unit path length. Niels Bohr was the first one [2] to evaluate the energy straggling per unit path,

$$\Omega_\infty^2 = 4\pi N_{\text{at}} Z_p^2 Z_T, \quad (1)$$

where Z_T and N_{at} are the atomic number and atomic density of the target, respectively. Ω_∞ is usually known as Bohr straggling. Since Ω_∞ is deduced on the assumption that all target electrons can be considered as free, it is expected to be valid in the high velocity limit. At low and intermediate impact velocities, deviations from the Bohr straggling Ω_∞ arise, and a detailed description of the involved energy-loss processes is necessary to calculate Ω .

In metallic solids we can separate the contributions to the straggling coming from collisions with valence- (Ω_V) and inner-shell (Ω_{IS}) electrons as

$$\Omega^2 = \Omega_V^2 + \Omega_{IS}^2. \quad (2)$$

At the considered energies the straggling produced by elastic collisions with target nuclei is negligible.

We evaluate the contribution coming from the valence band with the dielectric theory [3], while the energy straggling due to collisions with inner-shell electrons is calculated with an atomic collisional model. In previous works this last contribution has been evaluated by extending the response function of a free-electron gas to include bound electrons (local density approximation) [4,5], or by considering an atomic model represented by generalized oscillator strengths [6]. Details of the theoretical models employed in this work to describe Ω_V and Ω_{IS} are summed up below.

A. Valence contribution

We calculate the valence straggling Ω_V within the framework of the usual dielectric formulation [3,7,8], which yields

$$\Omega_V^2 = -\frac{2Z_P^2}{\pi v^2} \int_0^\infty \frac{dq}{q} \int_0^{vq} d\omega \omega^2 \text{Im} \left[\frac{1}{\epsilon(q, \omega)} \right], \quad (3)$$

where q and ω are the momentum and energy transfers, respectively, and $\epsilon(q, \omega)$ is the dielectric function of the solid. To describe $\epsilon(q, \omega)$ we used the Mermin-Lindhard approximation [9], which allows us to deal with finite values of the plasmon lifetime γ^{-1} .

On the other hand, the interaction with valence electrons involves two different mechanisms: the excitation of collective modes (plasmons), and the excitation of free electrons by binary collisions with the projectile. The energy straggling Ω_V given by Eq. (3) includes these two mechanisms without separating their contributions. However, as far as we deal with a free-electron gas, it is possible to decompose the valence straggling as $\Omega_V^2 = \Omega_{sp}^2 + \Omega_c^2$, where Ω_{sp} is the straggling produced by single-particle collisions, and Ω_c is the one originated by collective excitations [8,10]. The straggling contribution Ω_{sp} becomes

$$\Omega_{sp}^2 = -\frac{2Z_P^2}{\pi v^2} \int_0^\infty \frac{dq}{q} \int_0^{qv} d\omega \omega^2 \text{Im} \left[\frac{1}{\epsilon(q, \omega)} \right] \times \Theta(k_F^2 - B^2), \quad (4)$$

with $B = (\omega - q^2/2)/q$. Note that the Heaviside function $\Theta(k_F^2 - B^2)$ defines the binary region, where the two-particle system (projectile and active electron) conserves the energy. The straggling contribution of collective excitations Ω_c is obtained by subtracting Eq. (4) from Eq. (3), i.e., $\Omega_c^2 = \Omega_V^2 - \Omega_{sp}^2$. We must mention that Eq. (4) is exact when using the Lindhard dielectric function only. Nonetheless, the approximation is still valid for finite values of $\gamma \ll \omega_p$.

B. Inner-shell contribution

The energy dispersion per unit path produced by ionization from the initial bound state i , Ω_i , is given by [11]

$$\Omega_i^2 = \frac{(2\pi)^4 N_{\text{at}}}{v^2} \int d\mathbf{k}_f \int d\boldsymbol{\eta} \Theta(k_f - k_F) \omega_{if}^2 |T_{ik_f}|^2, \quad (5)$$

where \mathbf{k}_f is the final electron momentum, k_F is the Fermi momentum, and $\boldsymbol{\eta}$ is the transversal momentum transfer. The variable ω_{if} is the energy gained by the electron in the transition $i \rightarrow k_f$, and T_{ik_f} is the corresponding T -matrix element. Assuming that the nonionized core electrons remains “frozen” during the collision, the problem is reduced to one-active-electron system, and the Heaviside function $\Theta(k_f - k_F)$ imposes the Pauli exclusion principle.

To evaluate T_{ik_f} we employ the continuum-distorted-wave eikonal-initial-state (CDW-EIS) approximation, which is a quantum-mechanical method that considers the distortion of the electron waves produced by the projectile in the initial

and final channels of the collision. This method has been found to be successful in explaining the ionization process for a large variety of collision systems [12]. With the CDW-EIS model the T -matrix element reads

$$T_{ik_f}^{\text{CDW-EIS}} = \langle \chi_{k_f}^{\text{CDW}} | W_f^\dagger | \chi_i^E \rangle, \quad (6)$$

where $\chi_{k_f}^{\text{CDW}}$ is the final CDW wave function, which contains a product of two continuum states, one around the target and the other around the projectile, χ_i^E is the eikonal wave function, and W_f is the final perturbative potential. The total core contribution is obtained by adding over all occupied initial states, that is $\Omega_{IS}^2 = \sum_i \Omega_i^2$, where the index i denotes the different atomic inner-subshells.

III. EXPERIMENTAL PROCEDURE

As in the previous cases of Al, Zn, and Au targets [1], the straggling determinations for Si presented here were made by the transmission method. The self-supported (2 mm diameter) amorphous silicon foils were made by evaporation under clean vacuum conditions on a very smooth plastic substrate [13] which was subsequently dissolved. The foil thicknesses were determined by matching energy-loss measurements at higher energies (100 to 200 keV) with recent stopping cross-section determinations [14], yielding a value of 20 nm. An exhaustive analysis of the Si foils was performed, so that the impurity concentration, sample topography, and crystalline structure has been analyzed by Auger Electron Spectroscopy, AFM (atomic force microscopy), and TEM (transmission electron microscopy), respectively. The Auger spectroscopy revealed that the main impurities are carbon and oxygen with a total combined concentration of $\approx 10\%$. The AFM studies yielded a roughness coefficient ρ of 12%, with ρ defined as the variance of the foil thickness distribution relative to the mean foil thickness. This ρ value was corroborated by an *in situ* analysis using ion beams [15]. As TEM microscopy showed, the foils were amorphous with a high degree of uniformity and no pinholes were apparent.

The effect of the impurities has been evaluated using theoretical straggling values for O and C [16], yielding an effect of $\approx 2\%$ which lies well within the experimental uncertainties. The main factor affecting the measurements is the foil roughness. The present experimental data are corrected for this using the formula $\Omega^2 = \Omega_{\text{exp}}^2 - \rho^2 \Delta E^2$ [17], where Ω_{exp} is the measured straggling and ΔE is the measured energy loss. Because of the differences in the energy dependences of ΔE and Ω , the incidence of this roughness correction varies with the projectile energy. The values of the resulting corrections have been represented with error bars in the Figs. 2–5, and, as can be seen, they are more important at low energies.

More experimental details can be found in Ref. [1].

IV. RESULTS

We study the energy straggling for protons impinging on four different solids: Al, Si, Zn and Au. They are metals, with the only exception of Si which is a semiconductor with a

TABLE I. Parameters involved in the straggling of protons, in atomic units. Atomic number Z_T , atomic density N_{at} , number of electrons ceded to the free-electron gas n_V , and damping coefficient γ . Bohr's values of the valence (Ω_{∞_V}) and total (Ω_{∞}) straggling.

| | Z_T | $N_{\text{at}} (10^{-2})$ | n_V | γ | $\Omega_{\infty_V}^2$ | Ω_{∞}^2 |
|----|-------|---------------------------|-------|----------|-----------------------|---------------------|
| Al | 13 | 0.892 | 2.83 | 0.037 | 0.317 | 1.457 |
| Si | 14 | 0.74 | 4.21 | 0.156 | 0.372 | 1.302 |
| Zn | 30 | 0.974 | 3.2 | 0.4 | 0.392 | 3.68 |
| Au | 79 | 0.874 | 8.21 | 1.5 | 0.901 | 8.68 |

very small gap. The parameters used to describe these target materials are shown in Table I (see [18–20]).

We assume that target atoms cede n_V electrons (as given in Table I) from their outermost shells to the free-electron gas, keeping the remaining $Z_T - n_V$ electrons in bound levels. In the calculation of the inner-shell contribution the target cores are considered as isolated, and no correction is included to take into account that they are part of the solid. For Al, Si, and Zn, the bound states are described by Hartree-Fock functions [21] corresponding to the ions Al^{3+} , Si^{4+} , and Zn, respectively. In the case of Au, instead, hydrogenlike wave functions with effective charges (derived from Hartree-Fock eigenenergies [22]) are used. For all the targets, the final continuum state is represented as a Coulomb wave function with an effective charge corresponding to the binding energy. In the considered energy range, the contribution coming from the K shell can be neglected in the evaluation of the straggling because the ion velocity is not large enough.

To investigate the sources of the energy dispersion, in Fig. 1 we plot the partial contributions involved in the valence and inner-shell straggling, as a function of the impact energy. Two metal solids are considered, aluminum in Fig. 1(a) and zinc in Fig. 1(b). The valence contributions Ω_{sp}^2 and Ω_c^2 are displayed with solid lines, while the contributions from the different atomic subshells are plotted with dashed lines. At low energies, below the threshold of atomic ionization, only collisions with electrons of the conduction band contribute to the energy dispersion. And in this process, the binary collisions are the dominant mechanism, even above the threshold of collective excitations, which is determined by the velocity $v_{\text{th}} \approx \omega_p / q_c$ with $q_c = \sqrt{k_F^2 + 2\omega_p - k_F}$, where $\omega_p = (4\pi n_V N_{\text{at}})^{1/2}$ is the plasmon frequency. Contrary to the mean energy loss, where plasmon and single-particle contributions are of the same order (equipartition rule, in the high energy limit) [3], the collective straggling Ω_c^2 is negligible compared with Ω_{sp}^2 in the whole energy range considered. As an example, at 100 keV the single-particle and collective energy loss per unit path in Al are 0.149 and 0.056, respectively, while the corresponding values of straggling are 0.345 and 0.039. This result is a consequence of the presence of the factor ω^2 in Eq. (3), which reinforces the contribution of binary (head-on type) collisions. It is also in agreement with similar findings of Kimura *et al.* [23] in collisions with surfaces.

As the projectile velocity increases, the contribution of

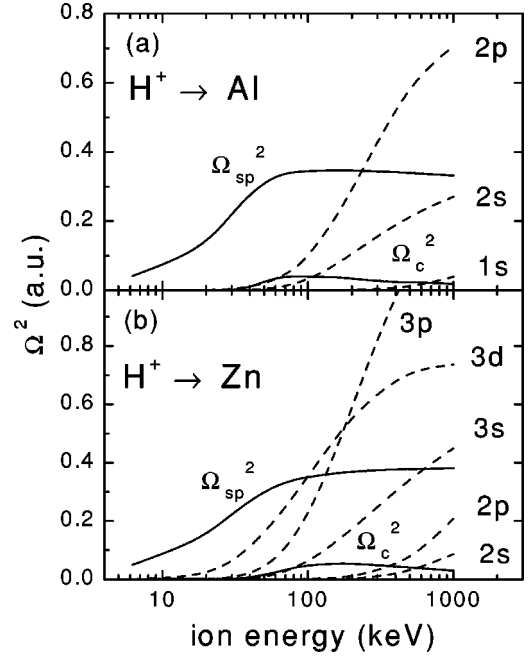


FIG. 1. Partial contributions to the energy straggling of protons in (a) Al and (b) Zn as a function of the impact energy. Solid lines, valence contribution from single-particle (sp) and collective (c) mechanisms; dashed lines, inner-shell contributions.

bound electrons starts to be relevant following a stripping scheme, i.e., from external to internal shells. At intermediate energies the external shells of the ionic cores are more easily ionized than the internal ones, while the lower states play a significant role in the higher velocity region. From Fig. 1(a) we observe that the energy straggling produced by ionization from the K shell is negligible, as mentioned above.

We have also studied the contribution to the energy straggling due to charge exchange processes by employing the eikonal impulse approximation [24]. In particular, for an aluminum target, the energy straggling produced by capture from inner shells of the target atoms is $\Omega_{\text{cap}}^2 = 0.019$ and 0.018 a.u. at 50 and 100 keV, respectively. These values are more than one order of magnitude lower than the valence contribution and decrease as the energy increases. Therefore, we have neglected charge exchange contributions in our calculations.

In Fig. 2 we plot our theoretical and experimental results of the energy straggling for silicon as a function of proton energy. The values are normalized to the Bohr value Ω_{∞} given by Eq. (1). To appreciate the energy range where each mechanism is important, partial contributions Ω_V/Ω_{∞} and $\Omega_{IS}/\Omega_{\infty}$ are also displayed in Fig. 2. At low impact energies the interaction with valence electrons is the dominant mechanism, but when the energy increases Ω_V/Ω_{∞} reaches a saturation value, and $\Omega_{IS}/\Omega_{\infty}$ starts to be relevant. The asymptotic limit of Ω_V for high velocities is obtained from Bohr's model by considering the interaction with conduction electrons only, which yields [25] $\Omega_{\infty_V} = Z_P \omega_p$. Bohr's predictions for valence and total straggling for $Z_P = 1$ are given in Table I. Since the vertical bars represent the corrections to

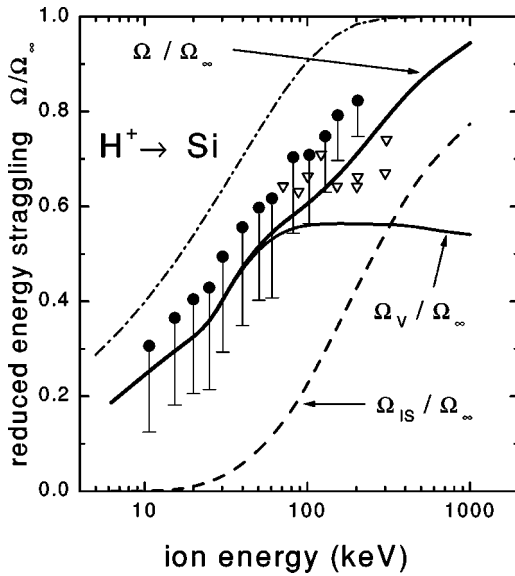


FIG. 2. Reduced energy straggling Ω/Ω_∞ for protons moving in Si as a function of the impact energy. Full circles, this experiment without foil roughness correction; negative error bars indicate the maximum possible foil roughness effect; open down-triangles, experimental data from Ref. [27]; dashed-dotted line, experimental fit from Ref. [14]; thick solid line, theoretical prediction of reduced energy straggling Ω/Ω_∞ ; thin solid and dash lines, theoretical values of the valence (Ω_V/Ω_∞) and inner-shell ($\Omega_{IS}/\Omega_\infty$) contributions, respectively.

the experimental data due to foil roughness [1], the agreement between theoretical and experimental values is considered good, especially at high energies. Other experimental values, obtained by Ikeda *et al.* [27] and corrected for the foil roughness effect, are also shown in Fig. 2, and a consistency of these data with our values is observed. A recent

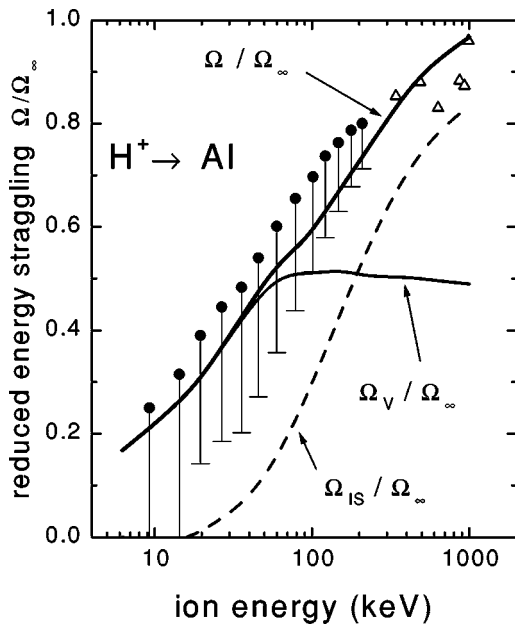


FIG. 3. The same as Fig. 2 for Al. Open up-triangles, experimental data from Ref. [26].

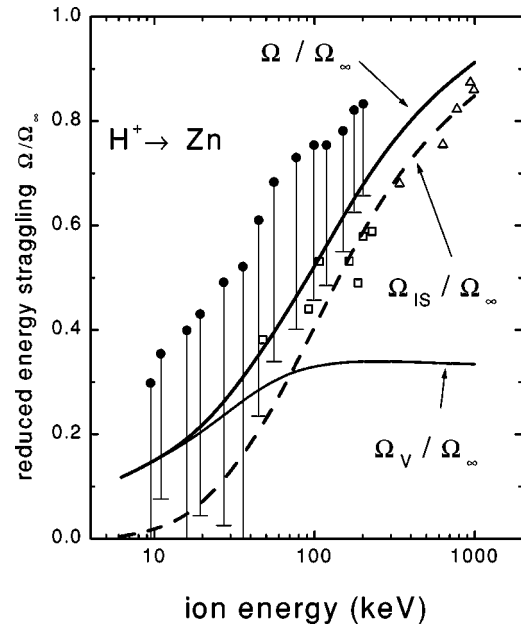


FIG. 4. The same as Fig. 2 for Zn. Open up-triangles, experimental data from Ref. [26]; open squares, experimental data from Ref. [28] for Cu.

experimental fit by Konac *et al.* [14], displayed as a dash-dotted line, yields higher values as compared with the present results.

Figures 3, 4, and 5 display the reduced energy straggling Ω/Ω_∞ as a function of the incident energy for Al, Zn, and Au targets, respectively. For these targets our theoretical predictions are compared with previous experimental data of Ref. [1]. As in the case of silicon, the collisions with valence-band electrons determine the energy dispersion at low velocities, while the interactions with the atomic cores provide an important contribution to Ω at high velocities. Taking into

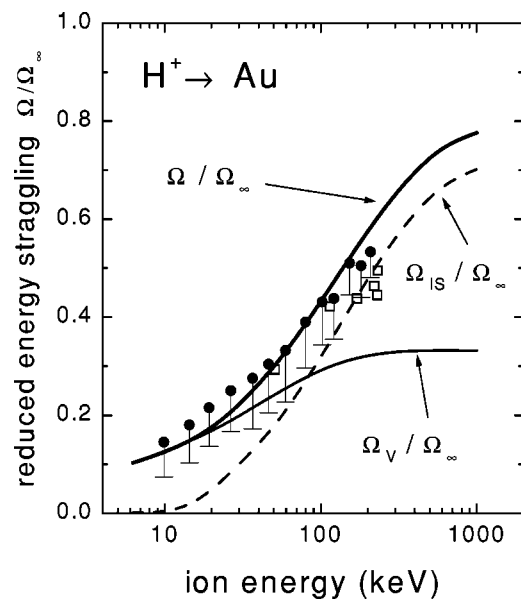


FIG. 5. The same as Fig. 2 for Au. Open squares, experimental data from Ref. [28] for Pt.

account the correction due to the foil roughness, the present theoretical results are in good agreement with the experimental data for Al and Zn, but they slightly overestimate the experiments for Au. For this case, we can mention two possible sources of error in our calculations. First, for gold we employ hydrogenlike functions with effective charges (instead of Hartree-Fock-Slater ones), and it is expected that the use of more appropriate wave functions gives a more precise value of the inner-shell contribution. And second, since Au has a high atomic number, its outermost atomic shells are easily ionized leading to a not-well-defined number of electrons n_V in the conduction band, and also to a high value of the inverse plasmon lifetime γ . Both factors introduce an additional uncertainty in the theoretical values of Ω_V . Experimental data measured by other authors are also included in the figures. In Fig. 3 for Al targets we compare our experimental results with previous data of Kido [26], obtained by using the nuclear resonance reaction technique. These data fit smoothly with our results at high impact velocities. To allow some further comparison with other experiments, data of the neighboring elements Cu and Pt [28] are also displayed in Figs. 4 (Zn) and 5 (Au), respectively.

V. CONCLUSIONS

We have presented a consistent method to evaluate the energy straggling of protons traveling through solids. This method is based on the separation of the contributions coming from valence and inner-shell electrons. The usual dielectric formalism with the Mermin prescription for the dielectric response function is used to account for valence straggling, while the CDW-EIS approximation is employed to describe the core ionization process.

The theoretical model is applied to the collisional systems composed of protons moving inside Al, Si, Zn, and Au solid targets, with intermediate and high velocities. For Al, Zn,

and Au, the theoretical results are compared with recent experimental data [1], while for Si new energy straggling measurements are presented. The experimental determinations have been performed with a straightforward procedure, the transmission method, and an exhaustive analysis of the Si-foil conditions has been carried out. Theoretical predictions are in good agreement with the experiments for Al, Si, and Zn. However, the model gives slightly higher values than the measured straggling for Au, and possible origins of this discrepancy have been put forward.

The different mechanisms involved in the energy dispersion are also investigated, and the collective excitation of valence electrons is found to have a minor influence in the energy straggling. The energy dispersion produced by single-particle collisions with valence electrons is the dominant contribution at low energies, reaching a saturation value when the velocity increases. On the contrary, inner-shell straggling becomes important at intermediate and high velocities; and core electrons belonging to outermost shells are more easily ionized than the internal ones.

We finally stress that, although straggling measurements are generally affected by larger uncertainties (mostly due to the target roughness effect) as compared to stopping power values, they show in a more direct way the various contributions of valence and inner shell electrons, in particular when the energy dependence is studied on a wide range. In this way, the analysis of straggling data yields an additional method of testing different theoretical models for the energy loss mechanism.

ACKNOWLEDGMENTS

This work was supported in part by the Argentine Conicet (project No. PIP 4267), the ANPCyT (projects No. PICT03-03579 and No. PICT03-06249) and UBACyT No. 01-X044.

-
- [1] J.C. Eckardt and G.H. Lantschner, Nucl. Instrum. Methods Phys. Res. B **175-177**, 93 (2001).
 - [2] N. Bohr, K. Dan. Vidensk. Selsk. Mat. Fys. Medd. **18**, 8 (1948).
 - [3] J. Lindhard, K. Dan. Vidensk. Selsk. Mat. Fys. Medd. **28**, 8 (1954).
 - [4] E. Bonderup and P. Hvelplund, Phys. Rev. A **4**, 562 (1971).
 - [5] W.K. Chu, Phys. Rev. A **76**, 2057 (1976).
 - [6] I. Abril, R. Garcia-Molina, N.R. Arista, and C.F. Sanz (unpublished).
 - [7] J. Lindhard and A. Winther, K. Dan. Vidensk. Selsk. Mat. Fys. Medd. **34**, No. 4 (1964).
 - [8] D.G. Arbó and J.E. Miraglia, Phys. Rev. A **58**, 2970 (1998).
 - [9] N.D. Mermin, Phys. Rev. B **1**, 2362 (1970).
 - [10] D.G. Arbó, M.S. Gravielle, and J.E. Miraglia, Phys. Rev. A **62**, 032901 (2000).
 - [11] M.S. Gravielle, Phys. Rev. A **62**, 062903 (2000).
 - [12] P.D. Fainstein, V.H. Ponce, and R.D. Rivarola, J. Phys. B **24**, 3091 (1991).
 - [13] A. Valenzuela and J.C. Eckardt, Rev. Sci. Instrum. **42**, 127 (1971).
 - [14] G. Konac, S. Kalbitzer, Ch. Klatt, D. Niemann, and R. Stoll, Nucl. Instrum. Methods Phys. Res. B **136-138**, 159 (1998).
 - [15] J.C. Eckardt and G.H. Lantschner, Thin Solid Films **249**, 11 (1994).
 - [16] J.F. Ziegler and W.K. Chu, At. Data Nucl. Data Tables **13**, 463 (1974).
 - [17] F. Besenbacher, J.U. Andersen, and E. Bonderup, Nucl. Instrum. Methods **168**, 1 (1980).
 - [18] D. Isaacson, New York University, Doc. No. 02698, National Auxiliary Publication Service (New York, 1975).
 - [19] N.R. Arista, Phys. Rev. A **49**, 1885 (1994).
 - [20] I. Abril, R. García-Molina, C.D. Denton, F.J. Pérez, and N.R. Arista, Phys. Rev. A **58**, 357 (1998).
 - [21] E. Clementi and C. Roetti, At. Data Nucl. Data Tables **14**, 177 (1974).
 - [22] T.A. Carlson, C.C. Lu, T.C. Tucker, C.W. Nestor, Jr., and F. B. Malik, Oak Ridge National Laboratory, Report No. ORNL-4614, 1970.

- [23] K. Kimura, H. Kuroda, M. Fritz, and M. Mannami, Nucl. Instrum. Methods Phys. Res. B **100**, 356 (1995).
- [24] M.S. Gravielle and J.E. Miraglia, Phys. Rev. A **44**, 7299 (1991).
- [25] P. Sigmund and K. Johannssen, Nucl. Instrum. Methods Phys. Res. B **6**, 486 (1985).
- [26] Y. Kido, Nucl. Instrum. Methods Phys. Res. B **24/25**, 347 (1987).
- [27] A. Ikeda, K. Sumimoto, T. Nishioka, and Y. Kido, Nucl. Instrum. Methods Phys. Res. B **115**, 34 (1996).
- [28] Y. Kido and T. Koshikawa, Phys. Rev. A **44**, 1759 (1991).